

OPTIMIZATION OF HIGHLY CIRCULARLY POLARIZED THERMAL RADIATION IN α -MoO₃/ β -Ga₂O₃ TWISTED LAYERS

Marco Centini^{1*}, Chiyu Yang², Maria Cristina Larciprete¹, Mauro Antezza^{3,4}, Zhuomin M. Zhang²

¹Sapienza University of Rome Department of Basic and Applied Sciences for Engineering,
Via A. Scarpa 14, I-00161 Rome, Italy

²George W. Woodruff School of Mechanical Engineering,
Georgia Institute of Technology, Atlanta, GA 30332, USA

³Laboratoire Charles Coulomb (L2C), UMR 5221 CNRS-Université de Montpellier,
F- 34095 Montpellier, France

⁴Institut Universitaire de France, 1 rue Descartes, F-75231 Paris Cedex 05, France

ABSTRACT. We investigate a bi-layer scheme for circularly polarized infrared thermal radiation. Our approach takes advantage of the strong anisotropy of low-symmetry materials such as β -Ga₂O₃ and α -MoO₃. We numerically report narrow-band, high degree of circular polarization (over 0.85), thermal radiation at two typical emission frequencies related to the excitation of β -Ga₂O₃ optical phonons. Optimization of the degree of circular polarization is achieved by a proper relative tilt of the crystal axes between the two layers. Our simple but effective scheme could set the basis for a new class of lithography-free thermal sources for IR bio-sensing.

1. INTRODUCTION

The development of miniaturized and integrable devices operating in the mid-infrared (mid-IR) relies on the availability of narrowband, highly directional, and polarization tunable sources. Indeed, several applications ranging from IR sensing [1,2] to biomedical diagnostics and target detecting [3,4] as well as for the realization of integrated IR photonics [5,6] require highly efficient, narrow-band, and polarization tunable mid-IR sources. An efficient but expensive option is represented by quantum cascade laser (QCL) IR sources. However, with the aim to achieve mass production of low-cost devices, a lot of research effort has been recently spent on the study of optimized and controllable thermal radiation sources. Thanks to the development of micro/nano technologies [7], several approaches to control and tailor the typically incoherent and broadband thermal radiation from heated bodies have been proposed and realized. The mechanism at the base of this tailored emission is the excitation of resonant states i.e. surface plasmon-(SP) or phonon-(SPh) polaritons, Bloch surface waves, magnetic polaritons, to name a few. Gratings [8], metamaterials [9,10], metasurfaces [11] and nanoantennae [12,13] have been successfully proposed to overcome and enhance the performances of natural bulk materials. However, all these approaches rely on the use of lithographic techniques to artificially create absorption/emission resonances as well as a strong birefringent effective response. In particular, birefringence is necessary for polarization sensitive applications.

An extreme form of birefringent behavior is called hyperbolicity and it is achieved when one diagonal element of the material dielectric tensor is negative, whilst the others are positive [14]. Hyperbolic metamaterials obtained by periodic sub-wavelength patterned layered media have been studied for enhanced thermal radiation and nanoscale heat transfer [15,16]. However, it has been recently

* Corresponding Author: marco.centini@uniroma1.it

shown that hyperbolicity can be observed in natural materials, more specifically in van der Waals (vdW) materials IR [17]. Among vdW materials, hexagonal boron nitride hBN is one of the most investigated [18]. The hBN exhibits two different Reststrahlen bands (negative values of the real part of the permittivity) along either the in-plane or out-of-plane directions. The main limitation of hBN is the lack of in-plane anisotropy. In-plane anisotropy is required to distinguish and manipulate orthogonal polarization states of the electromagnetic field at normal incidence.

Among the vdW polar materials displaying in-plane anisotropy, molybdenum trioxide (α -MoO₃) has been the object of a conspicuous number of recent studies [19,20]. Its strong anisotropy, allowing in-plane and off-plane hyperbolicity, has been used to obtain mid-IR waveplates [21] and tunable [22] and broadband [23] absorption in the far-field. Concerning the excitation of surface waves, hyperbolic phonon polaritons have recently been shown in α -MoO₃ flakes from 818 cm⁻¹ to 974 cm⁻¹ [20,24]. Furthermore, the excitation of SPh polaritons waves in twisted flakes of 2D α -MoO₃ has been proposed and experimentally verified [25]. Such control of SPh polaritons in twisted flakes has interesting applications for tunable near-field radiative heat transfer [26] by adjusting the tilt angle between the receiver and the emitter. It has been shown that twisted α -MoO₃ layers can exhibit circular dichroism [27,28] and can be used to generate spin thermal radiation [29]. However, using twisted structures of identical anisotropic materials to achieve spin thermal radiation has more restrictions on the materials. For this reason, α -MoO₃ was combined with an ideal quarter wavelength plate [29]. However, a tunable combination of two real anisotropic materials (i.e. controlling the tilt angle between them) could be adopted for practical applications and for integrated thermal sources.

Low-symmetry materials have recently emerged as possible candidates for anisotropic optical applications [30]. Among them, β -Ga₂O₃ [31,32] has been used to experimentally demonstrate the excitation of shear phonon polaritons in the IR [33,34]. Moreover, this material perfectly matches the usable wavelength range of α -MoO₃. More specifically we will show that there are phonon resonances in the β -Ga₂O₃ which fall in an almost transparent but highly anisotropic band of the α -MoO₃. Thus, we propose a combination of two twisted layers obtained from these two materials.

Our calculations, based on a complete Stokes parameters analysis [35] of emitted radiation, show that it is possible to obtain circularly polarized thermal radiation in the mid-IR with a twisted bilayer system having about two microns of total thickness. As a starting point we study the emission properties and the birefringence behavior of single layers of α -MoO₃ and β -Ga₂O₃ on gold substrates. The choice of gold substrate allows for an almost one-sided emissivity as long as we can ignore thermal emission for the gold back face in the mid-IR. After the choice of one of the two materials as the emitter, we add a properly tilted and sized layer of the other, acting as a quarter wave plate to obtain thermally radiated circularly polarized light.

2. NUMERICAL METHODS

In order to quantitatively study the degree of polarization (DoP) and the degree of circular polarization (DoCP) of the Thermal radiation polarization properties can be characterized by Stokes parameters. For reciprocal materials, the Stokes parameters can be expressed in terms of the polarized emissivities as [35,36]:

$$\begin{bmatrix} S_0 \\ S_1 \\ S_2 \\ S_3 \end{bmatrix} = \frac{S_{0,bb}(\omega, k_{\parallel})}{2} \begin{bmatrix} \epsilon_p + \epsilon_s \\ \epsilon_p - \epsilon_s \\ \epsilon_{45^\circ} - \epsilon_{135^\circ} \\ \epsilon_R - \epsilon_L \end{bmatrix}; \quad (1)$$

where $k_{//}$ is the wave vector projection onto the surface (x - y) plane, $S_{0,bb}$ is the emissivity of the black body, $\epsilon_{p,s}$ are the p - and s - polarized relative emissivities, $\epsilon_{45^\circ,135^\circ}$ are the 45° - and 135° - polarized relative emissivities and $\epsilon_{R,L}$ are the *right*- and *left*- circular polarized relative emissivities respectively. Limiting our discussion to reciprocal media at thermal equilibrium, polarized emissivities can be evaluated by calculating the polarized absorptivities α , according to Kirchoff's law:

$$\epsilon_{p,s,45^\circ,135^\circ,R,L} = \alpha_{p,s,45^\circ,135^\circ,R,L} \quad (2)$$

Polarized absorptivities have been retrieved by evaluating $1-R-T$ where R is reflectance and T is transmittance evaluated for the different polarized states of the incident light with a 4×4 transfer matrix method [37]. The degree of polarization (DoP) and the degree of circular polarization (DoCP) are then defined as:

$$\text{DoP} = \frac{\sqrt{S_1^2 + S_2^2 + S_3^2}}{S_0}; \quad (3)$$

$$\text{DoCP} = \frac{|S_3|}{S_0}; \quad (4)$$

Being both DoP and DoCP limited in the range $[0,1]$ and $\text{DoCP} \leq \text{DoP}$. $\text{DoP}=1$ stands for perfectly polarized light, thus $\text{DoCP}=1$ corresponds to perfectly circularly polarized light.

Our approach is based on the combination of two layers on top of gold substrate. The bottom layer acts as an emitter while the second acts as a quarter-wave plate. Both layers are required to be strongly anisotropic, however, the emitting layer should provide high emission/absorption efficiency for only one polarization component while the upper one should be as transparent as possible with a strong anisotropic real part of the refractive index. A particle swarm optimization is used as the search algorithm for the optimal parameters including the geometrical parameters (thickness) and the arrangement of the optic axes with the relative tilt angle between the two layers. In order to reduce the number of optimization parameters for the two-layer system the particle swarm algorithm is performed in two separate steps. At first, we set as the objective function the maximum degree of polarization (DoP) of the single, bottom, layer on gold. This way we find the layer thickness and emission wavelength for maximized DOP. Then we optimize the thickness and the relative orientation of the second (upper) layer to obtain maximum DoCP. We focus on the fact that this two-step optimization is performed to reduce the number of simultaneous sweeping parameters but it does not affect the accuracy of numerical results. Indeed, the adopted 4×4 transfer matrix model takes into account for multiple reflections. A complete single-step full sweep could lead to improved performances at a slightly shifted emission line. Nevertheless, we expect that this shift, typically related to multiple reflections, could play a relevant role in multilayer stacks or high-Q cavities, here we only focus on the double-layer scheme.

3. MATERIALS OPTICAL PROPERTIES

We study both α - MoO_3 and β - Ga_2O_3 optical properties in the mid-IR with the aim of identifying the frequency ranges where they can be efficiently combined. To begin with, we focus our study on the thermal radiation emitted along the direction normal to the surface. Thus, if we consider the x - y plane as the surface plane, the emission direction is toward the z -axis. We also select the orientation of the crystals so that x - and y - axes coincide with the x' - and y' - crystal axes. In this case, we are interested in the in-plane values of the dielectric permittivities. In Figure 1(a,b), the imaginary part of xx , yy and xy

components of the relative permittivity tensor of α -MoO₃ and β -Ga₂O₃ are plotted as a function of the frequency [20,38]. The imaginary part of the dielectric function is related to absorption/emission. For α -MoO₃, there are two main peaks at 550 cm⁻¹ and 820 cm⁻¹ due to optical phonons while for β -Ga₂O₃, there are three main bands centered around 570 cm⁻¹, 690 cm⁻¹ and 740 cm⁻¹, respectively. As previously mentioned, in our emitter/waveplate approach we want to avoid overlaps in the emission bands in order to clearly distinguish the role of the emitter from the role of the waveplate. For this reason, we exclude from further investigation the lower frequencies (570 cm⁻¹ and 550 cm⁻¹). In Figure 1(c), the real part of the refractive index components n_x and n_y α -MoO₃ and their $\Delta n = n_x - n_y$ are shown. The real part of the dielectric function components of β -Ga₂O₃ are shown in Figure 1(d). We note that α -MoO₃ has a wide band (from 600 cm⁻¹ to 750 cm⁻¹) of high and almost constant anisotropy which makes it very suitable to be used as a waveplate. Thus we focus our attention on the design of an efficient β -Ga₂O₃ emitting layer around 690 cm⁻¹ and 740 cm⁻¹ with a high DoP combined with a properly tilted and sized α -MoO₃ layer acting as waveplate to obtain a tailored thermal source with optimized DoCP.

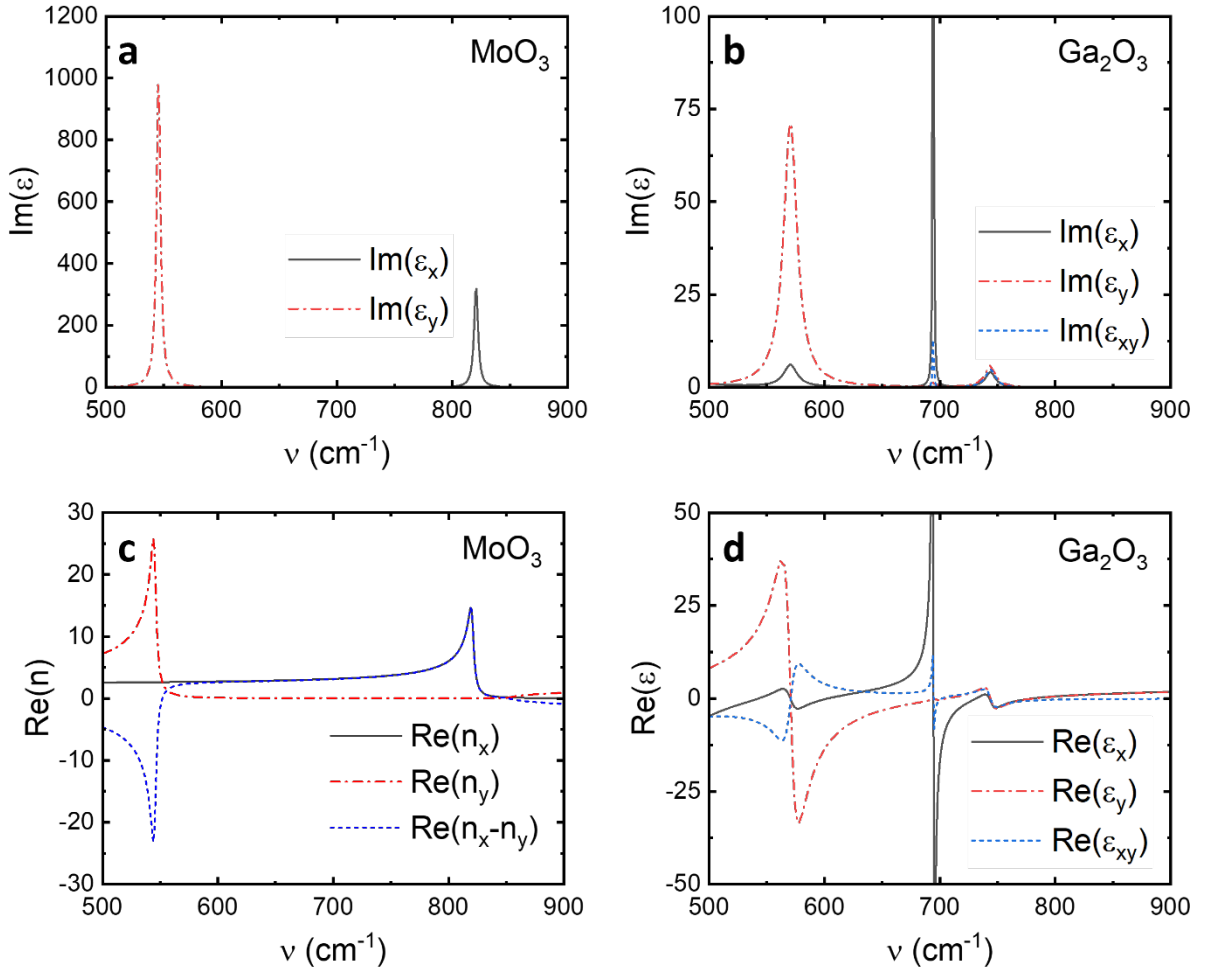


Figure 1. Imaginary part of the in-plane components (xx,xy,yy) of the dielectric permittivity tensor of (a) MoO₃, (b) Ga₂O₃. Real part of the refractive indices along x (n_x) and y (n_y) directions and Δn for (c) MoO₃ and Real part of the relative permittivity for (d) Ga₂O₃.

4. RESULTS AND DISCUSSION

We employed particle swarm optimization (PSO), a search algorithm that finds optimal solutions by iteratively trying to improve candidate solutions, and finally obtained structures with the highest circular emission at specific frequencies. The first optimization is performed on a single β -Ga₂O₃ layer on gold substrate. We found two schemes corresponding to maximized DoP at two different frequencies: 691 cm⁻¹ and 737 cm⁻¹. In the first scheme, sketched in Figure 2a, we note that a 606 nm thick β -Ga₂O₃ layer has a maximum relative emissivity for a p-polarized field at 691 cm⁻¹ corresponding to a DoP of about 0.97 and zero DoCP (Figure 2b). On the other hand, the second proposed scheme, sketched in Figure 2c is based on a thicker Ga₂O₃ layer (1909 nm) showing a maximum DoP=0.93 at ν =737 cm⁻¹. The main difference with respect to the previous case is that the initial DoCP is now about 0.1 (figure 2d). Thus the emitted radiation from the single Ga₂O₃ layer is elliptical.

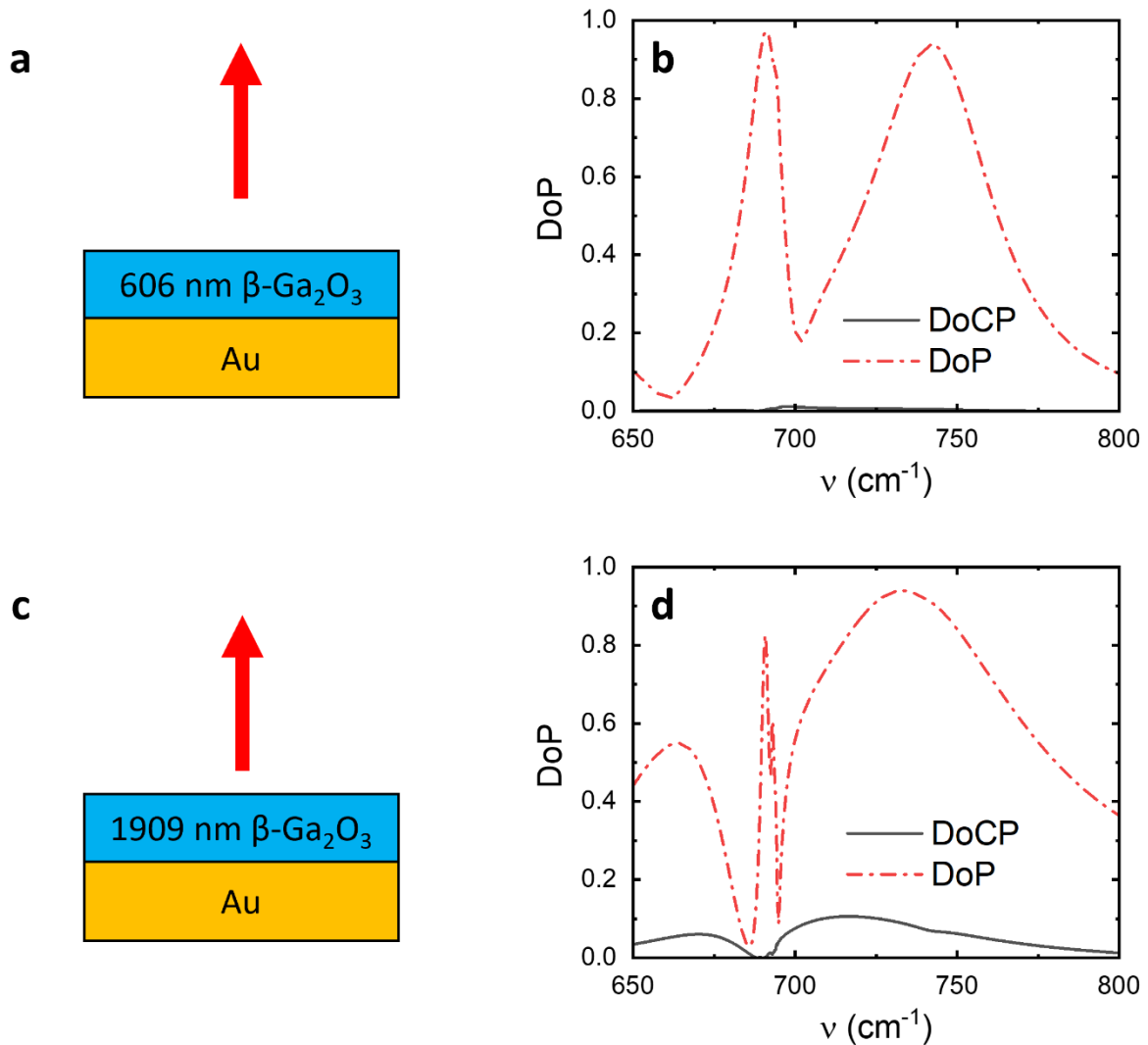


Figure 2. (a) Schematic of a single β -Ga₂O₃ layer exhibiting optimized DoP at ν =691 cm⁻¹; (b) DoP and DoCP as a function of the frequency for the system sketched in (a); (c) Schematic of a single β -Ga₂O₃ layer exhibiting optimized DoP at ν =737 cm⁻¹; (d) DoP and DoCP as a function of the frequency for the system sketched in (c).

Then we added a MoO₃ cap layer to both schemes and applied a second PSO varying the thickness and the relative orientation with respect to the bottom layer. For the first scheme we found an optimal condition corresponding to a DoCP=0.87 at 691 cm⁻¹ when a 740 nm α -MoO₃ layer, tilted by an angle of 83° in the x - y plane with respect to the $x'y'$ axes of the β -Ga₂O₃ layer is considered (sketch of figure 3a). All the results have been obtained with the indirect method, (i.e., calculating the absorptivity and applying Kirchhoff's law) and validated by the direct method based on fluctuation electrodynamics [35]. Figure 3b shows a high peak of almost left circularly polarized (LCP) emission at $\nu=691$ cm⁻¹. The corresponding DoP and DoCP are reported in Figure 3c. We note that DoP=DoCP=0.87 at nearly the same frequency (see Figure 3c). Finally, we report in Figure 3d the value of S₃/S₀ as a function of the twist angle between the two layers and of the frequency. Its modulus is the DOCP, however, its sign determines the Right (if positive) or Left (if negative) circular polarization. The reported map clearly shows that at $\nu=691$ cm⁻¹ it is possible to switch from almost perfect (DoCP=0.87) RCP to LCP by properly tuning the twist angle.

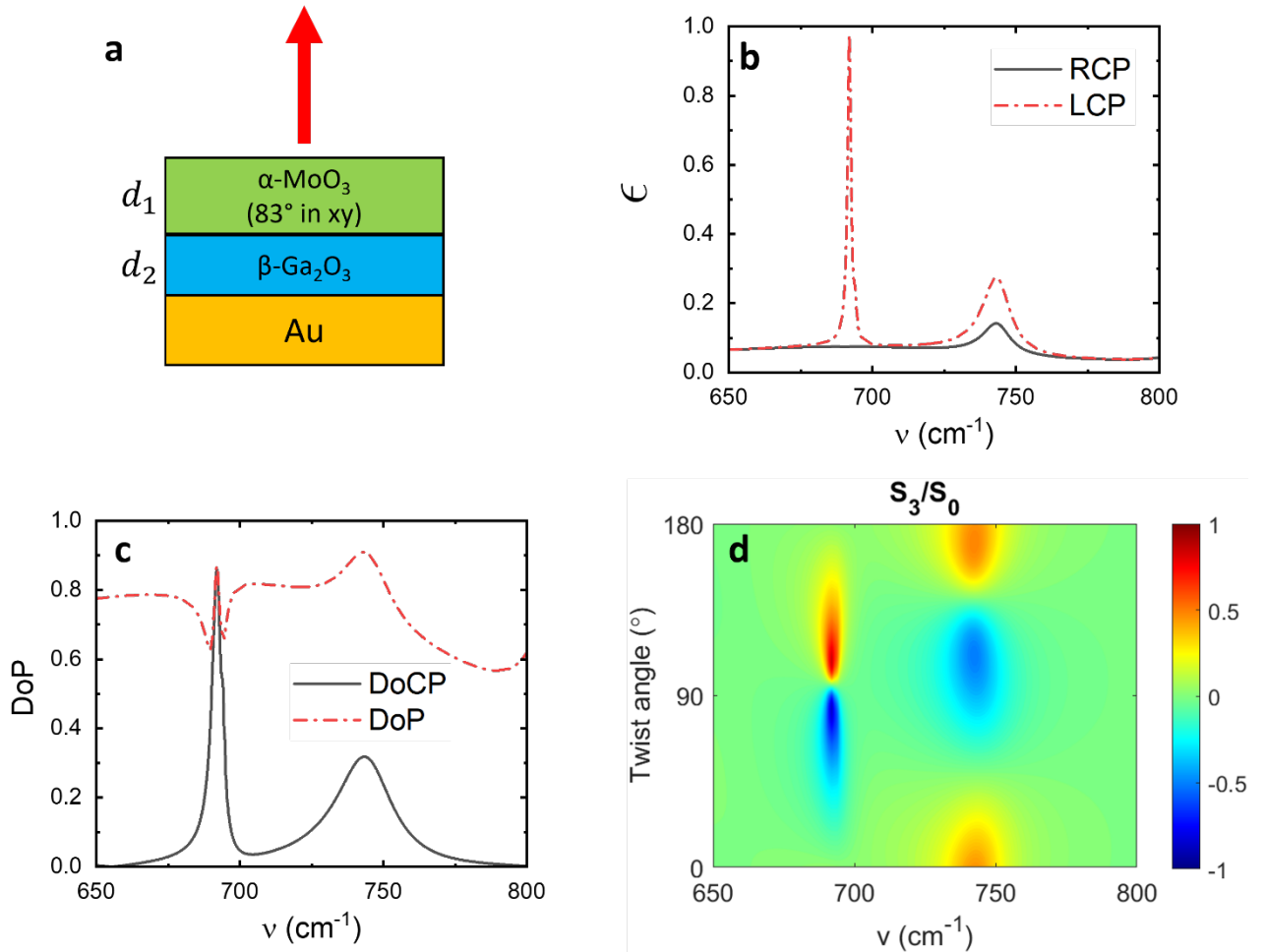


Figure 3. (a) Schematic of twisted bi-layer structure designed for $\nu=691$ cm⁻¹, obtained by adding a α -MoO₃ layer on top of the β -Ga₂O₃ layer; (b) circularly polarized emissivity and (c) degree of polarization of the twisted bi-layer structure; (d) S₃/S₀ as a function of the twist angle and of the frequency. We note

that by proper tuning of the twist angle it is possible to switch from LCP to RCP emission at $\nu=691\text{ cm}^{-1}$.

A similar performance is achieved for the second scheme adding a 324 nm thick layer of $\alpha\text{-MoO}_3$ as sketched in Figure 4a, rotated in the $x\text{-}y$ plane of 114° with respect to the $x'y'$ axes of the $\beta\text{-Ga}_2\text{O}_3$ layer. We note that in this case, we obtain a resulting $\text{DoP} = \text{DoCP} = 0.85$ (figure 4c) and the thermal emitted radiation at 737 cm^{-1} is mostly left circularly polarized (figure 4b). However, right-hand circular polarization at 737 cm^{-1} can be obtained similarly to the previous scheme, by varying the twist angle of the MoO_3 layer as shown in Figure 4d.

We finally explore the robustness of the proposed schemes by varying the emission angle i.e. the Azimuth angle (ϕ) and Zenith angle (θ) to show that the results are maintained over a large angular range for both schemes (Figure 5a and 5b respectively).

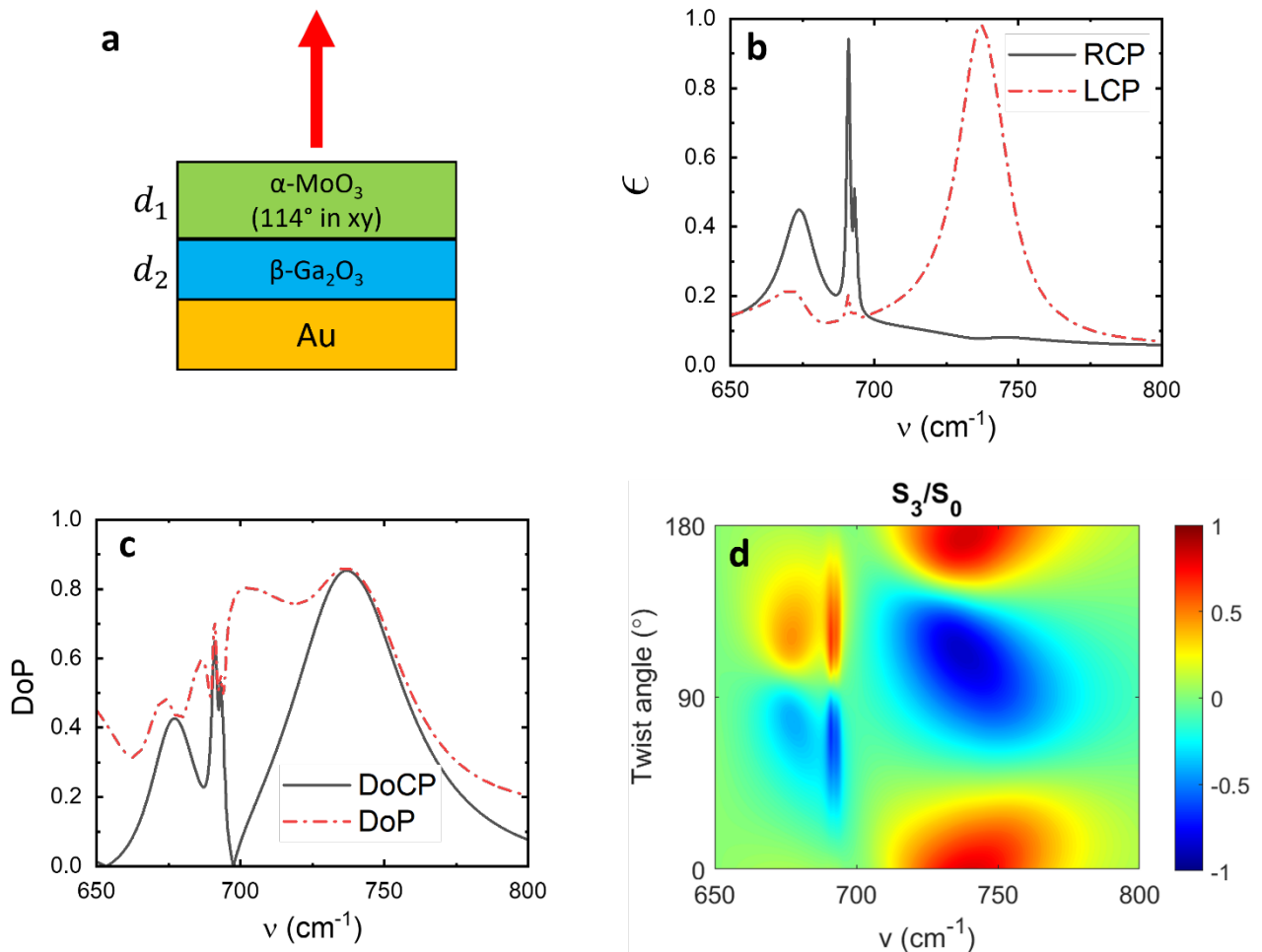


Figure 4. (a) Schematic of twisted bi-layer structure designed for $\nu=737\text{ cm}^{-1}$, obtained by adding a $\alpha\text{-MoO}_3$ layer on top of the $\beta\text{-Ga}_2\text{O}_3$ layer; (b) circularly polarized emissivity and (c) degree of polarization of the twisted bi-layer structure; (d) S_3/S_0 as a function of the twist angle and of the frequency. We note that by proper tuning of the twist angle it is possible to switch from LCP to RCP emission at $\nu=737\text{ cm}^{-1}$.

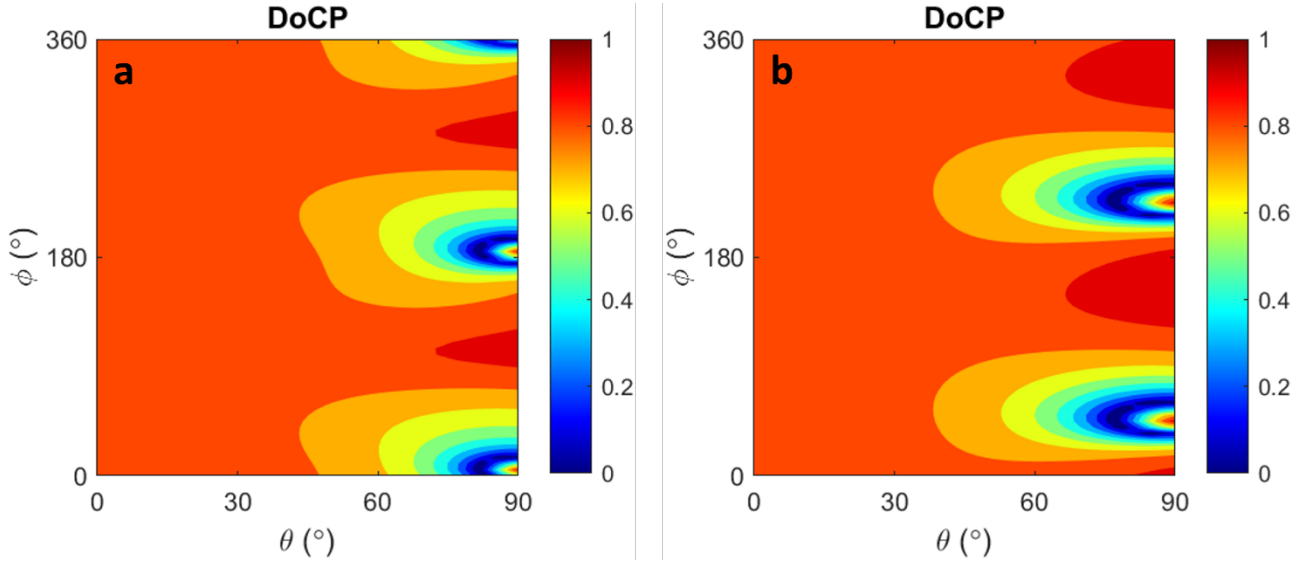


Figure 5. DoCP of thermal radiation emitted (a) at $\nu=691 \text{ cm}^{-1}$ for the structure sketched in figure 3a and (b) at $\nu=737 \text{ cm}^{-1}$ for the structure sketched in figure 4a as a function of angle (ϕ) and Zenith angle (θ).

Further evidence of the robustness of the bi-layer approach is reported in Figure 6. We performed single parameters sweep (on Ga_2O_3 layer and on MoO_3 layer thickness) around the optimal conditions for scheme 1 (Figure 6 a,b) and scheme 2 (Figure 6 c,d). We show that high degree of circular polarization is maintained over a large range of the thickness of the layers corresponding to hundreds of nm. We note that scheme 1 allows for a narrow band emission with a good tunability of 5 cm^{-1} , varying the thickness of the Ga_2O_3 layer and maintaining a DoCP higher than 0.7. On the other hand, scheme 2 emits on a larger bandwidth and it is extremely robust with respect to tolerances on the layer's thickness.

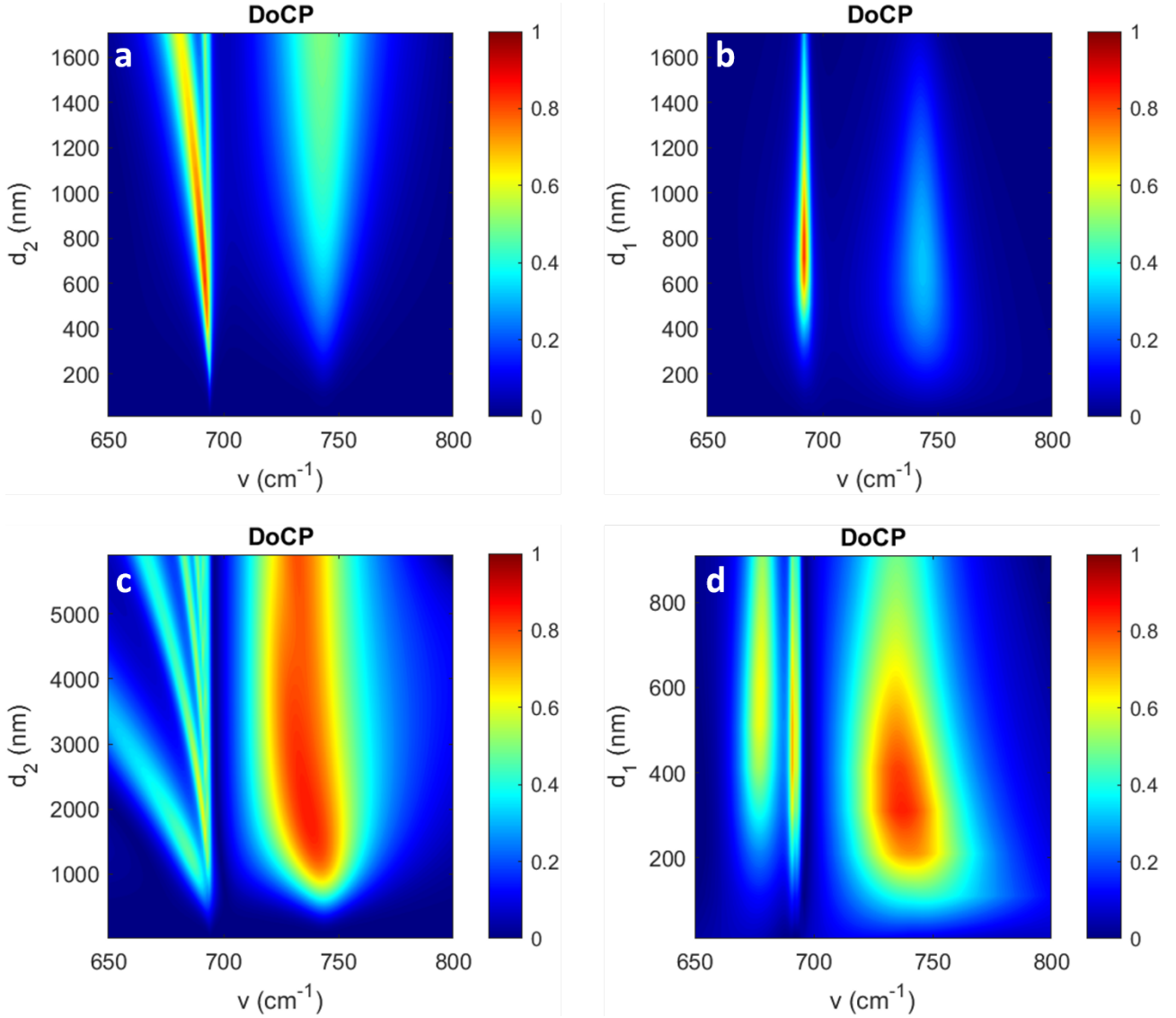


Figure 6. DoCP as a function of the frequency and the (a) β -Ga₂O₃ layer thickness, (b) α -MoO₃ layer thickness for scheme 1. DoCP as a function of the frequency and the (c) β -Ga₂O₃ layer thickness, (d) α -MoO₃ layer thickness for scheme 2.

5. CONCLUSION

We proposed a lithography-free method based on a double-twisted layer scheme to obtain circularly polarized thermal radiation in the mid-IR, at two specific frequencies related to β -Ga₂O₃ optical phonons excitation. The almost linearly polarized emission from the single slab is converted into circular polarization by adding a properly sized and tilted α -MoO₃ layer acting as a quarter-wavelength plate. In both cases, we take advantage of the strong natural anisotropy related to the low symmetry class of the investigated materials without the need for further processing techniques. The achieved degree of circular polarization is higher than 0.85 for the two proposed schemes and it is maintained over a broad range of angles of emission. We believe that this approach could lead to the development of low-cost, integrated thermal sources of circularly polarized light for IR sensing applications.

ACKNOWLEDGEMENT

M.A. thanks the SAPIENZA University of Rome and the Department of Basic and Applied Sciences for Engineering for hospitality during his stay in Rome under the visiting professor program, where this work has been initiated. M.C, M.C.L, M.A. and Z.M.Z. acknowledge the KITP program ‘Emerging Regimes and Implications of Quantum and Thermal Fluctuational Electrodynamics’ 2022, where part of this work has been done. This research was supported in part by the National Science Foundation under Grant No. PHY-1748958. C.Y. was supported by the National Science Foundation (CBET-2029892).

REFERENCES

- [1] J. Hodgkinson and R. P. Tatam, “Optical gas sensing: a review,” *Meas. Sci. Technol.* 24(1), 012004, 2013 (**Journal Paper**)
- [2] R. Furstenberg, C. A. Kendziora, J. Stepnowski, S. V. Stepnowski, M. Rake, M. R. Papantonakis, V. Nguyen, G. K. Hubler, and R. A. McGill, “Stand-off detection of trace explosives via resonant infrared photothermal imaging,” *Appl. Phys. Lett.* 93(22), 224103 2008 (**Journal Paper**)
- [3] M. F. Wood, D. Côté, and I. A. Vitkin, “Combined optical intensity and polarization methodology for analyte concentration determination in simulated optically clear and turbid biological media,” *J. Biomed. Opt.* 13(4), 044037, 2008. (**Journal Paper**)
- [4] F. Snik, J. Craven-Jones, M. Escuti, S. Fineschi, D. Harrington, A. D. Martino, D. Mawet, J. Riedi, and J. S. Tyo, in *Polarization: Measurement, Analysis, and Remote Sensing XI*, Vol. 9099, edited by D. B. Chenault and D. H. Goldstein, International Society for Optics and Photonics (SPIE, 2014) p. 90990 (**Conference Proceedings**)
- [5] Y. Chen, Y. Francescato, J. D. Caldwell, V. Giannini, T. W. W. Maß, O. J. Glembocki, F. J. Bezares, T. Taubner, R. Kasica, M. Hong, and S. A. Maier, “Spectral Tuning of Localized Surface Phonon Polariton Resonators for Low-Loss Mid-IR Applications,” *ACS Photonics* 1(8), 718–724, 2014. (**Journal Paper**)
- [6] J.D. Caldwell et al. Low-loss, infrared and terahertz nanophotonics using surface phonon polaritons. *Nanophotonics* 4, 44–68, 2015. (**Journal Paper**)
- [7] Z. M. Zhang, *Nano/Microscale Heat Transfer*, 2nd ed. (Springer, 2020). (**Book**)
- [8] J.-J. Greffet, R. Carminati, K. Joulain, J.-P. Mulet, S. Mainguy, and Y. Chen, “Coherent emission of light by thermal sources,” *Nature* 416(6876), 61–64, 2002. (**Journal Paper**)
- [9] M. C. Larciprete, M. Centini, R. Li Voti, and C. Sibilia, “Selective and tunable thermal emission in metamaterials composed of oriented polar inclusions,” *J. Opt. Soc. Am. B* 34(7), 1459–1464, 2017. (**Journal Paper**)
- [10] A. Lochbaum, Y. Fedoryshyn, A. Dorodnyy, U. Koch, C. Hafner, and J. Leuthold, “On-Chip Narrowband Thermal Emitter for Mid-IR Optical Gas Sensing,” *ACS Photonics* 4(6), 1371–1380 (2017). (**Journal Paper**)
- [11] A. C. Overvig, S. A. Mann, and A. Alù, “Thermal Metasurfaces: Complete Emission Control by Combining Local and Nonlocal Light-Matter Interactions”, *Phys. Rev. X* 11, 021050, 2021 (**Journal Paper**)
- [12] M. Centini, M. C. Larciprete, R. Li Voti, M. Bertolotti, C. Sibilia, and M. Antezza, "Hybrid thermal Yagi-Uda nanoantennas for directional and narrow band long-wavelength IR radiation sources," *Opt. Express* 28, 19334-19348, 2020 (**Journal Paper**)
- [13] C. Li, V. Krachmalnicoff, P. Bouchon, J. Jaeck, N. Bardou, R. Haïdar, and Y. De Wilde, “Near-Field and Far-Field Thermal Emission of an Individual Patch Nanoantenna,” *Phys. Rev. Lett.* 121(24), 243901, 2018 (**Journal Paper**)
- [14] A. Poddubny, I. Iorsh, P. Belov, & Y. Kivshar, “Hyperbolic metamaterials”, *Nat. Photon.* 7, 948, 2013. (**Journal Paper**)
- [15] S. Campione, F. Marquier, J.-P. Hugonin, A. R. Ellis, J. F. Klem, M. B. Sinclair, and T. S. Luk, “Directional and monochromatic thermal emitter from epsilon-near-zero conditions in semiconductor hyperbolic metamaterials,” *Sci. Rep.* 6(1), 34746, 2016. (**Journal Paper**)
- [16] C. Simovski, S. Maslovski, I. Nefedov, and S. Tretyakov, “Optimization of radiative heat transfer in hyperbolic metamaterials for thermophotovoltaic applications,” *Opt. Express* 21(12), 14988–15013. 2013. (**Journal Paper**)
- [17] Q. Zhang, G. Hu, W. Ma, P. Li, A. Krasnok, R. Hillenbrand, A. Alù, and C.-W. Qiu, “Interface nano-optics with van der Waals polaritons,” *Nature* 597(7875), 187–195, 2021 (**Journal Paper**)
- [18] J.D. Caldwell, I. Aharonovich, G. Cassabois, et al. “Photonics with hexagonal boron nitride”. *Nat Rev Mater* 4, 552–567, 2019. (**Journal Paper**)
- [19] G. Álvarez-Pérez, T. G. Folland, I. Errea, J. Taboada-Gutiérrez, J. Duan, J. Martín-Sánchez, A. I. F. Tresguerres-Mata, J. R. Matson, A. Bylinkin, M. He, W. Ma, Q. Bao, J. I. Martín, J. D. Caldwell, A. Y. Nikitin, and P. Alonso-González, “Infrared Permittivity of the Biaxial van der Waals Semiconductor α -MoO₃ from Near- and Far-Field Correlative Studies,” *Adv. Mater.* 32(29), 1908176, 2020. (**Journal Paper**)

- [20] Z. Zheng, N. Xu, S. L. Oscurato, M. Tamagnone, F. Sun, Y. Jiang, Y. Ke, J. Chen, W. Huang, W. L. Wilson, A. Ambrosio, S. Deng, and H. Chen, "A mid-infrared biaxial hyperbolic van der Waals crystal," *Sci. Adv.* 5(5), eaav8690, 2019. **(Journal Paper)**
- [21] S. Abedini Dereshgi, T. G. Folland, A. A. Murthy, X. Song, I. Tanriover, V. P. Dravid, J. D. Caldwell, and K. Aydin, "Lithography-free IR polarization converters via orthogonal in-plane phonons in α -MoO₃ flakes," *Nat. Commun.* 11(1), 5771, 2020. **(Journal Paper)**
- [22] S. Abedini Dereshgi, M. C. Larciprete, M. Centini, A. A. Murthy, K. Tang, J. Wu, V. P. Dravid, and K. Aydin, "Tuning of Optical Phonons in α -MoO₃-VO₂ Multilayers," *ACS Appl. Mater. Interfaces* 13(41), 48981–48987, 2021. **(Journal Paper)**
- [23] G. Deng, S. Abedini Dereshgi, X. Song, C. Wei, and K. Aydin, "Phonon-polariton assisted broadband resonant absorption in anisotropic α -phase Mo O₃" nanostructures", *Phys. Rev. B* 102(3), 035408, 2020. **(Journal Paper)**
- [24] Maria Cristina Larciprete, Sina Abedini Dereshgi, Marco Centini, and Koray Aydin, "Tuning and hybridization of surface phonon polaritons in α -MoO₃ based metamaterials," *Opt. Express* 30, 12788-12796, 2022. **(Journal Paper)**
- [25] G. Hu, Q. Ou, G. Si, Y. Wu, J. Wu, Z. Dai, A. Krasnok, Y. Mazor, Q. Zhang, Q. Bao, C.-W. Qiu, and A. Alù, "Topological polaritons and photonic magic angles in twisted α -MoO₃ bilayers," *Nature* 582(7811), 209–213, 2020 **(Journal Paper)**
- [26] X. Wu, C. Fu, and Z. M. Zhang, "Near-Field Radiative Heat Transfer Between Two α -MoO₃ Biaxial Crystals," *J. Heat Transfer* 142(7), 072802, 2020. **(Journal Paper)**
- [27] B-Y. Wu et al, "Strong chirality in twisted bilayer α -MoO₃" 2022 *Chinese Phys. B* 31 044101 **(Journal Paper)**
- [28] B-Y. Wu, M. Wang, F. Wu, and X. Wu, "Strong extrinsic chirality in biaxial hyperbolic material α -MoO₃ with in-plane anisotropy," *Appl. Opt.* 60, 4599-4605, 2021. **(Journal Paper)**
- [29] P. Liu, L. Zhou, J. Tang, B-Y. Wu, H. Liu, and X. Wu, "Spinning thermal radiation from twisted two different anisotropic materials," *Opt. Express* 30, 32722-32730, 2022. **(Journal Paper)**
- [30] W. Ma, P. Alonso-González, S. Li, A. Y. Nikitin, J. Yuan, J. Martín-Sánchez, J. Taboada-Gutiérrez et al. "In-plane anisotropic and ultra-low-loss polaritons in a natural van der Waals crystal"; *Nature* 562, no. 7728, 557-562, 2018. **(Journal Paper)**
- [31] F.K Urban, D. Barton, and M. Schubert. "Numerical ellipsometry: A method for selecting a near-minimal infrared measurement set for β -gallium oxide", *Journal of Vacuum Science & Technology A: Vacuum, Surfaces, and Films* 39, no. 5: 052801, 2021. **(Journal Paper)**
- [32] M. Zhao, R. Tong, X. Chen, T. Ma, J. Dai, J. Lian, and J. Ye. "Ellipsometric determination of anisotropic optical constants of single phase Ga₂O₃ thin films in its orthorhombic and monoclinic phases" *Optical Materials* 102: 109807, 2020. **(Journal Paper)**
- [33] N.C. Passler, X. Ni, G. Hu, et al. Hyperbolic shear polaritons in low-symmetry crystals. *Nature* 602, 595–600, 2022. **(Journal Paper)**
- [34] C-L Zhou, G. Tang, Y. Zhang, M. Antezza, and H-L Yi , "Radiative heat transfer in a low-symmetry Bravais crystal", *Phys. Rev. B* 106, 155404, 2022 **(Journal Paper)**
- [35] C. Yang, W. Cai, and Z. M. Zhang, "Polarimetric analysis of thermal emission from both reciprocal and nonreciprocal materials using fluctuation electrodynamics", *Phys. Rev. B* 106, 245407, 2022 **(Journal Paper)**
- [36] F. Marquier, C. Arnold, M. Laroche, J. J. Greffet, and Y. Chen, *Opt. Express* 16, 5305, 2008 **(Journal Paper)**
- [37] N. C. Passler & A. Paarmann, "Generalized 4×4 matrix formalism for light propagation in anisotropic stratified media: study of surface phonon polaritons in polar dielectric heterostructures" *J. Opt. Soc. Am. B* 34, 2128–2139, 2017 **(Journal Paper)**
- [38] M. Schubert, R. Korlacki, S. Knight, T. Hofmann, S. Schöche, et al. "Anisotropy, phonon modes, and free charge carrier parameters in monoclinic β -gallium oxide single crystals" *Phys. Rev. B* 93, 125209, 2016 **(Journal Paper)**